Soft Matter

Dynamic Article Links

Cite this: *Soft Matter*, 2011, **7**, 9283

www.rsc.org/softmatter

PAPER

Protein molecule stratification inside a single curved film: Evidence from X-ray scattering

Janine Emile,*[a] Stéphane Pezennec,[bc] Anne Renault,[a] Estelle Robert,[a] Franck Artzner,[a] Cristelle Meriadec,[a] Alain Faisant[a] and Florian Meneau[d]

Received 31st May 2011, Accepted 1st July 2011
DOI: 10.1039/c1sm06010d

We have studied single curved films stabilized by globular proteins, using small angle scattering. By combining both the use of in-house X-ray and synchrotron radiation, we have measured the structural properties of films (thickness, electronic density) by controlling the physicochemical properties of protein (ovalbumin, pH 7, bulk concentration 10 g L^{-1}). For each experiment, solutions of highly purified protein were freshly prepared to eliminate any problem of aging. The observation of Kiessig fringes shows that the films are thin with an average thickness of 60 nm. Benefiting from the fine angular resolution and the short acquisition time of a synchrotron source, we have highlighted a stratification formation inside the films. This phenomenon suggests protein structural reorganization under confinement, possibly driven by high osmotic pressure.

1. Introduction

An aqueous foam is a dispersion of gas bubbles separated by thin liquid films, stabilized by amphiphilic molecules, especially proteins in the food industry.[1] The foam stability is largely determined by the drainage and coalescence (the breakdown of the bubbles by film rupture). A good knowledge of the structure of these films is essential for controlling the formation and stability of foams. Many studies have been focussed on the interfacial properties of proteins adsorbed at the air/solution interface[2–4] and single foam films.[5–9] The foams are stabilised by proteins adsorbing strongly to the air/solution interface, forming viscoelastic layers. Environmental and processing factors, such as temperature, pH, protein concentration, ionic strength and foam generation (whipping, bubbling) alter the physicochemical and conformational properties (size, shape, charge distribution, *etc.*) and the stability of proteins, and therefore, affect film formation and their properties.[1] For our studies, we were interested in the foaming ability of ovalbumin (the major egg-white protein) as a model system. The physicochemical and structural characteristics of this globular protein are known,[10] and the behaviour of ovalbumin at the air/solution interface has been extensively studied.[11–13] The aging of the interfacial film has been correlated with the development with time of a β-sheet network.[13] The formation of intermolecular disulfide bonds has been highlighted after foaming,[14] showing that ovalbumin undergoes conformational changes during foam formation. However, the behaviour of ovalbumin inside a film (thin liquid layers bounded by two air/solution interfaces) and the relationship between its structural and interfacial properties are not known.

In such a context, we have performed small angle X-ray scattering (SAXS) experiments on ordered foams. The simplest structure corresponds to the bamboo foams formed by an equal spacing of parallel films (Fig. 1). This can be generated in a narrow tube, where the bubbles are identical and of a size close to the diameter of the tube.[15] Relative to the orientation of the tube (vertical or horizontal), we have observed two categories of liquid films: films perpendicular to the wall of the tube and the wetting film. The junction between them is ensured by the Plateau border corresponding to a meniscus surrounding the circumference of the tube. Experiments concerning the drainage have shown an unusual behavior:[16] the shape of the Plateau border cross-section can strongly influence the flow in the wetting film. In the extreme case (tube radii less than $0.918\ell_c$, ℓ_c capillary length of the foam solution), drainage is not observed and the wetting film does not seem to ensure the connection between various films constituting the bamboo foam anymore. Unlike studies of disordered 3D foams,[17–20] the film orientation with respect to the beam may overcome some problems with the data analysis, such as the contribution of the Plateau border accidentally contaminating the pattern, or the contribution of several films of different thicknesses giving an averaged signal. Moreover, SAXS experiments should be preferred to neutron ones,

[a]*Institut de Physique de Rennes, UMR6251 UR1-CNRS, Université de Rennes 1, Bât 11 A, Campus de Beaulieu, 35042 Rennes Cedex, France. E-mail: janine.emile@univ-rennes1.fr; Fax: +33 2 23 23 67 17; Tel: +33 2 23 23 56 46*
[b]*INRA, UMR1253 Science et Technologie du Lait et de l'Œuf, F-35042 Rennes, France*
[c]*AGROCAMPUS OUEST, UMR1253 Science et Technologie du Lait et de l'Œuf, F-35042 Rennes, France*
[d]*Beamline SWING, Synchrotron SOLEIL, BP 48, 91192 Gif-sur-Yvette, France*

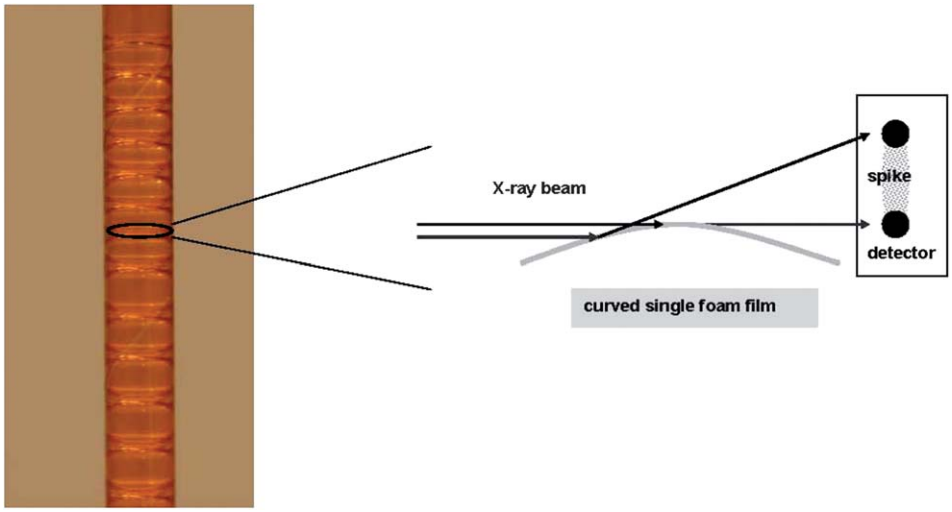

Fig. 1 A schematic description of the experimental conditions. The left photo shows a bamboo foam. Right, a zoom of the experimental set up showing the reflections of parallel X-ray beams by a curved interface of the film (for clarity, the film curvature is exaggerated). To simplify the scheme, interferences within the film have not been drawn.

since in neutron diffraction, the beam size is larger (about 1 cm). This requires the foam films to be stabilized in a tube of comparable diameter (bad quality produced foam).[21] For X-ray experiments, the samples could be smaller (one order of magnitude lower). Specifically, a synchrotron source allows high resolution spectra to be obtained in a short acquisition time (about one second), which eliminates any problem of protein aging. To demonstrate the feasibility of this approach, studies on the bamboo foam of SDS (sodium dodecyl sulfate), whose physicochemical behavior is well known, have previously been performed.[21,22] The main objective here is to investigate the structural properties of well controlled protein films.

2. Experimental procedures

Ovalbumin was extracted from hen egg white by anion-exchange chromatography.[23] Protein solutions were prepared just before the beginning of the experiments by solubilizing the lyophilized protein in 50 mM Bis-Tris propane buffer (2,2′-(propane-1,3-diyldiimino)bis[2-(hydroxymethyl)propane-1,3-diol]), (Sigma-Aldrich, St-Quentin Fallavier, France), pH 7 and ionic strength $I = 88.7$ mM. The 10 g L^{-1} protein solution was filtered (0.22 μm) to remove any insoluble material. The bulk protein concentration was chosen in order to obtain stable films. If the concentration is lower than 3 g L^{-1}, the films break. For a concentration higher than 30 g L^{-1}, aggregates formed in the films generate peaks in the SAXS spectra, whose position is random from one film to another. This point will be discussed below.

Bamboo foams were prepared in a 4 mm diameter Kapton tube.[21,22] The tube was set on the top of a syringe, and a small amount of solution was poured into it. Stable foams were obtained by bubbling air gently in the solution and tilting the tube (the bubbling velocity and tilt angle determine the geometry of the foam). Both sides of the tube were closed with caps which induce a pressure difference on both sides of the film, generating a small curvature of the film. Instead of studying a single isolated film, we chose a film among others within the foam (Fig. 1). As the tube radius is close to the capillary length ℓ_c (in our case $\ell_c = 2.1$ mm), the bamboo foam is simply an assembly of independent films.

In-house X-ray measurements were performed in the Institut of Physics of Rennes (IPR, Rennes, France) using a rotating anode X-ray generator FR591 (Brucker, Courtaboeuf, France) operated at 50 kV and 50 mA, giving a monochromatic radiation ($\lambda = 1.54$ Å). Patterns were collected with a Mar345 Image-Plate detector (Maresearch, Norderstedt, Germany). Additional information is given elsewhere.[22] The sample to detector distance was 449 mm and the X-ray patterns were recorded for a range of reciprocal spacing $q = 4\pi \sin\theta/\lambda$ from 0.2–15 nm^{-1} where θ is the diffraction angle. The acquisition time was typically 15 min in order to have a good signal-to-noise ratio. The experimental room was air conditioned at 20 °C.

Synchrotron experiments were performed on beamline SWING at SOLEIL (Gif-sur-Yvette, France) with a 12 keV beam ($\lambda = 1.0332$ Å) with a cross section 50 μm × 300 μm^2. The sample to AVIEX CCD detector distance was 1.552 m (q range between 0.04 to 5 nm^{-1}) and the acquisition time was 10 ms. The temperature of the experimental room was not controlled and was rather high (at least 25 °C); the lifetime of the foam was short (of the order of 10 min). The influence of the temperature on the foaming properties is not simple.[24] In addition to drainage and collapse, high temperatures ($T > 25$ °C), may impact the protein stability. However, experimental results obtained at IPR and SOLEIL are in agreement with each other and rule out temperature effects on the experimental spectra.

For each set of experiments (in-house X-ray and synchrotron), we used freshly prepared solutions of purified proteins and buffers. Before doing any data acquisition on ovalbumin films, adjustments were made on a SDS film, which is now the standard sample. The beam position on a film needs accurate adjustments to fulfil reflectivity requirements. We have used a camera to visualize the film that was slid into the tube and we have performed XZ scans to collect the best signal. The adjustment time of the experimental setup could last at least ten minutes, which

suggests that the foam has totally drained. Some experiments were made after slightly shaking the tube to evacuate some liquid. The SAXS instrumental resolution allows the film thicknesses to be measured below 500 nm.

The two-dimensional data were processed by the FIT2D software.[25] Non-linear fittings were performed using KaleidaGraph (Synergy Software, Reading, PA, USA).

3. Results

The scattering pattern (Fig. 2) is composed of two contributions: an isotropic one and an anisotropic one.[22] The isotropic contribution, which has the shape of circular halos, comes mainly from the Kapton tube. The other contribution, illustrated by a spike, is due to the specular reflection of the parallel X-ray beam on the curved film surface. The isotropic contribution was measured in the angular part without the spike and was then subtracted from the whole signal, to extract information on thickness and structure. We have obtained a specular reflectivity profile in the shape of oscillations superimposed with a q^{-4} decay, the so-called Kiessig fringes.

Unlike in a classical reflectivity experiment for which the incidence angle θ varies, *in situ* measurements performed on a film directly depend on its curvature (Fig. 1). The intrinsic curvature of the film is a major parameter in the experiment. We could obtain the angular distribution by a single acquisition. The curvature radius R of a film inside a drained foam was estimated at 0.15 m.[21] With a 4 mm diameter tube containing the bamboo foam, the angle dispersion $\Delta\theta = D/R$, with D the tube diameter, is 1.5° (*i.e.* $\Delta q = 1.6$ nm^{-1}), which is compatible with the SAXS spike length. Additional measurements in a horizontal position were made showing that the film remains flat, giving a single spot in the diffraction pattern corresponding to the specular reflectivity. Such motionless reflectivity experiments have already been proposed for Langmuir layers.[26] The main advantage is the quick experimental acquisition time, that ensures the absence of structural evolution during the reflectivity acquisition. Moreover, this setup does not require a long alignment procedure for the planar film orientation, which is very obvious in the case of films.

Fig. 2 represents an in-house X-ray scattering map. One can see a vertical spike whose intensity is modulated. The other, more diffuse, spike (above the beamstop) seems to come from the bulk scattering in the liquid phase of the Plateau border (menisci) that is much thicker. Integration of the data along the well-defined spike (Fig. 3) shows an abnormally high

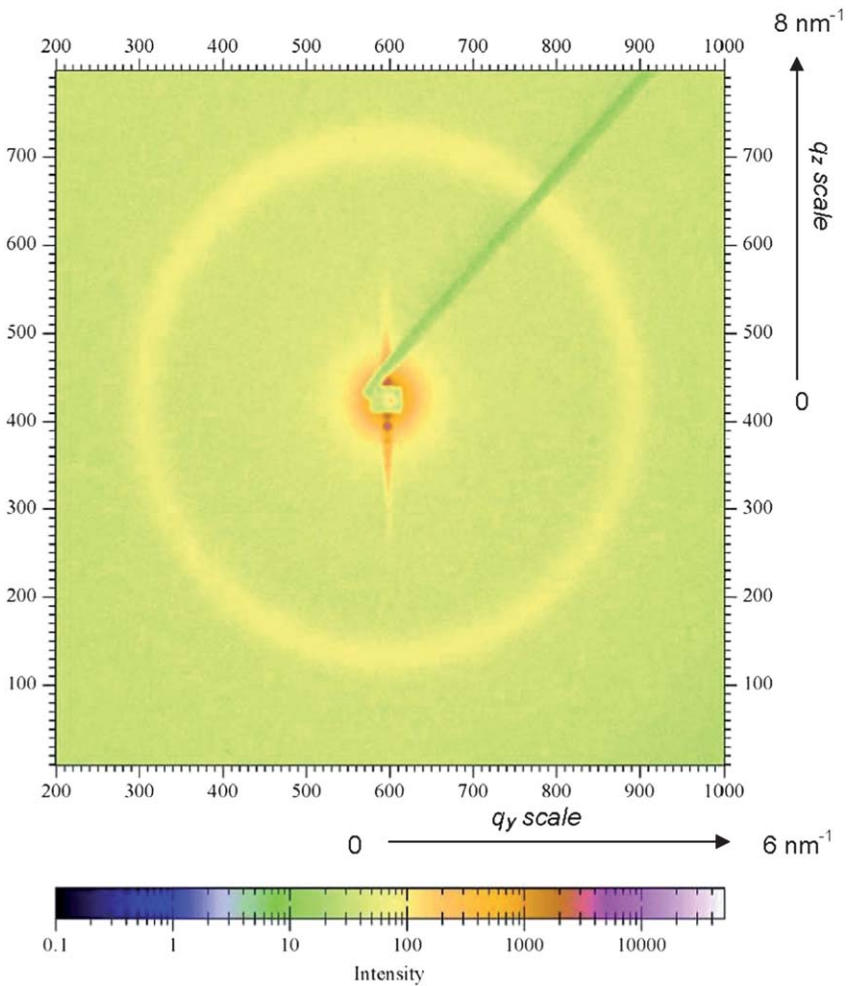

Fig. 2 An example of an X-ray pattern (IPR, Rennes) recorded for an ovalbumin film (visualization by FIT2D software).

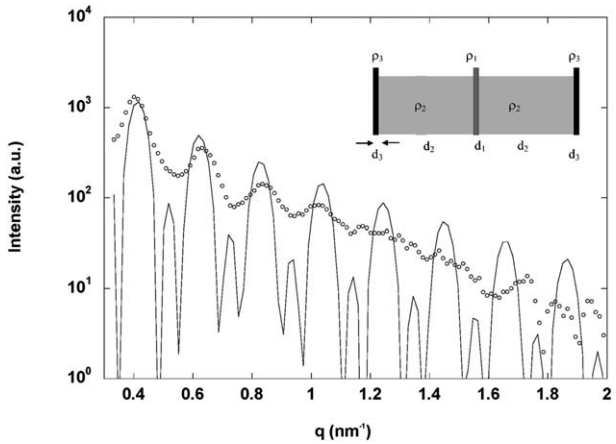

Fig. 3 The integration of X-ray experimental data along the spike, by subtracting the contribution of the kapton tube (open circle). The plain line corresponds to a fit with a "five-layer" model. Inset: schematic of the electron density profile of the film composed with five layers.

background scattering. The oscillations are broad with minima that do not reach zero. This shows that, unlike in SDS films,[20–22] the ovalbumin film seems to have a more complex structure. In particular, fitting the electronic density using the "three-layer" model (two surfactant layers at the air/solution interface and a solution slice) is clearly not appropriate. A better resolution in q (here 0.15 nm^{-1}) is needed to fit the data and to extract the possible presence of hidden oscillations in the background. In this context, we performed experiments using the high flux of the synchrotron and its fine angular resolution.

Fig. 4 is an example of a synchrotron pattern recorded on the detector of the SWING beamline at SOLEIL. Two spikes with different profiles are observed. The intensity in the "lower" spike with a q^{-4} decay is not modulated: its origin may be attributed to the liquid menisci characterized by two interfaces of opposite curvature. It was useless to select another film from the foam, since the high temperature generated a systematic breakdown of the films above the film studied. The meniscus in contact with the tube wall is swollen with solution. The "upper" spike presents two specific behaviours: well-defined oscillations coming from the film and an intense peak centred at 2.4 nm^{-1} ("Bragg peak") (Fig. 5). Several measurements on different films have been made to ensure the reproducibility of data. Scans along the film thickness (longitudinal scans) and along the film plane (transverse scans) must be performed to observe the "Bragg peak", to intersect the Ewald sphere. The background suddenly falls to zero for $q = 3$ nm^{-1}. The asymmetry of the spectrum may come from the surface texture of the film resulting from the formation of a rigid gel network or superimposed base line due to the Kiessig fringes.

3.1 Kiessig fringes

A "five-layer" model was selected to fit the Kiessig fringes (inset of Fig. 3). The film is described by two layers of solution (thickness d_2, electronic density ρ_2) separated by a layer with a different electron density (thickness d_1, electronic density ρ_1). Both air/solution interfaces of the film are composed by two layers consisting of a protein adsorption layer (thickness d_3, electronic density ρ_3). Within a kinematical approximation, the

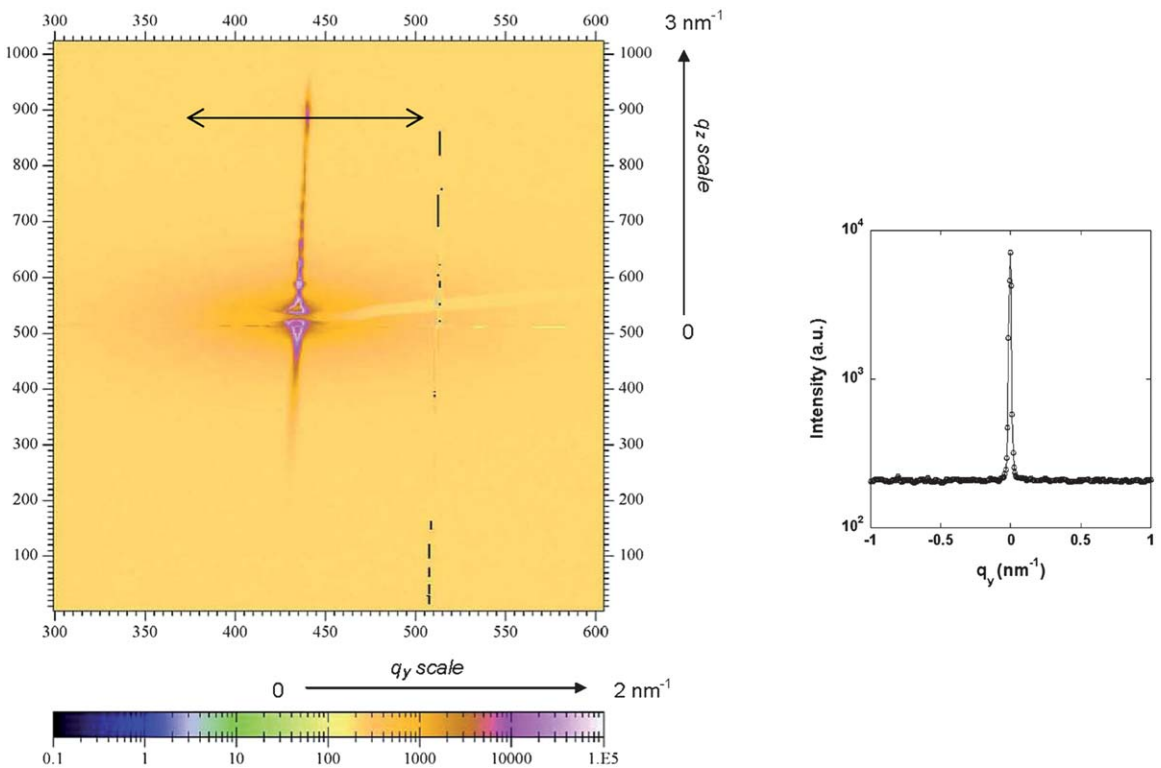

Fig. 4 An example of a synchrotron pattern (SOLEIL, Gif-sur-Yvette) recorded for an ovalbumin film. The cross represents the intersection of four detectors. The arrow shows a q_y scan across the spike; the integrated intensity is drawn on the right.

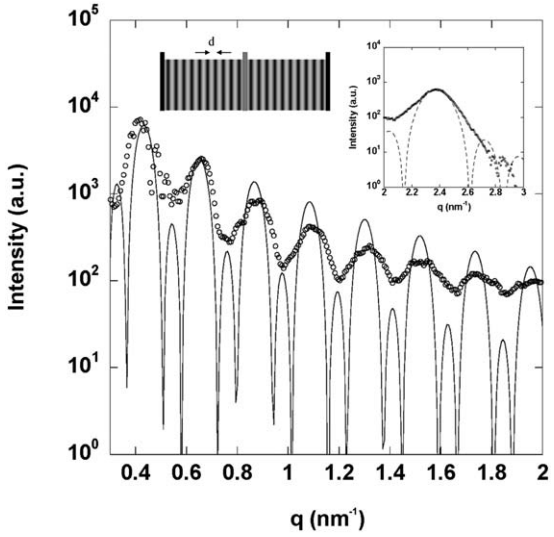

Fig. 5 The integration of synchrotron experimental data along the spike, by subtracting the contribution of the kapton tube (open circle). The plain line corresponds to the fit of this data with a "five-layer" model. The "Bragg peak" contribution is illustrated by the dotted line. Insert: the "Bragg peak" described by the Laue function; schematic of the electron density profile of the film with a stratification inside the layers denoted 2.

specular reflectivity intensity averaged on the coherence of the beam is given by[27–29]:

$$R(q) = R_F(q)\ |\Phi(q)|^2\ \mathrm{CW}(q, T, \gamma) \quad (1)$$

where R_F is the Fresnel reflectivity for an ideally flat interface,

$$R_F(q) = \frac{(4\pi r_0)^2}{q^4} \quad (2)$$

and r_0 is the classical electron radius. $|\Phi(q)|^2$ is the intrinsic structure factor normal to the surface, which is expressed as:

$$|\Phi(q)|^2 = \left|\frac{1}{\rho^\infty}\int \mathrm{d}z \frac{\mathrm{d}\langle\rho(z)\rangle}{\mathrm{d}z} \mathrm{e}^{\mathrm{i}qz}\right|^2 \quad (3)$$

ρ_∞ is the bulk electron density and $\langle\rho(z)\rangle$ is the average electron density profile normal to the surface, $\mathrm{CW}(q,T,\gamma)$ is the surface roughness term due to capillary waves and depends on the surface tension γ and the temperature T. It is given by:

$$\mathrm{CW}(q,T,\gamma) = \mathrm{e}^{(-\sigma^2(\gamma,T)q^2)} \quad (4)$$

where the surface roughness σ (characteristic length scale), which is about a few Å at room temperature, is neglected here for SAXS experiments since the resolution is much lower than the resolution of reflectivity experiments.[27]

The reflectivity formula derived from the Fourier transform of uniform electron densities in each layer enables us to use analytical functions in a reasonable simplified model:

$$R(q) \approx \frac{64\pi^2 r_0^2}{q^4}\left[\begin{array}{l}(\rho_1-\rho_2)\sin\left(\frac{qd_1}{2}\right)+(\rho_2-\rho_3)\sin\left(\frac{qd_1}{2}+qd_2\right)\\ +\rho_3\sin\left(\frac{qd_1}{2}+qd_2+qd_3\right)\end{array}\right]^2 \quad (5)$$

To interpret the small angle scattering data, we must introduce a geometric factor in the formula (5), which takes into account the film curvature. Nevertheless, this parameter is small[22] and does not influence the description of the oscillations.

In-plane wavelength dependence of the roughness (off-specular reflectivity or diffuse scattering) should be included in the X-ray data. However, this contribution is generally present for a larger q range with a high resolution reflectivity diffractometer adapted to perform surface-diffraction scans.[30] Transverse q_y cuts for different q_z points of the spike (Fig. 4) only show that the profile is defined by the instrumental resolution. We did not observe any profile broadening in our data, confirming that the diffuse scattering contribution can be neglected.

To limit the number of fitting parameters (here 7 parameters) of the formula (5), we have made several assumptions: the electronic density ρ_2 is set to 1 (reference), layers in the periphery of the film and the interior are assumed to be identical ($d_1 = d_3$, $\rho_1 = \rho_3$). The latter assumption is only meaningful if the layers are thin. Regarding the "reference" layer, we have assumed *a priori* that it is mainly composed of water because of the low protein concentration. Thus, the only fitting parameters are the absolute intensity scaling factor, d_1, ρ_1, d_2. The model was fitted to the data using the Levenberg–Marquardt algorithm. A statistical weighting was introduced, which gave more weight to highest intensity values, that is, first oscillations and tops of the last oscillations.

3.2 "Bragg peak"

Diffuse scattering centred at 2.4 nm^{-1}, labelled (00ℓ) "Bragg peak", could be simply described by the Laue function $\left(\sin\left(\frac{Nqd}{2}\right)/\sin\left(\frac{qd}{2}\right)\right)^2$ where N is the number of proteins ordered within the film with a periodicity d (insert of Fig. 5). The value of $qd/2$ corresponding to (00ℓ) "Bragg peak" is $\ell\pi$ and in the reflectivity pattern, the Laue function is divided by q^2. The description of this diffraction contribution is independent of the one used for Kiessig fringes, allowing us to simplify the model. The existence of a "Bragg peak" reveals electronic density fluctuations within the layers, perpendicular to the film surfaces. The peak position is defined by the periodicity of the alignment, which is found at 2.64 ± 0.01 nm for (001) "Bragg peak" ($\ell = 1$). The width is given by the number of proteins, which is found to be $N = 10 \pm 1$ within each thick layer. Given the particular variation of the background, it is not possible to define more precisely the number of proteins N. To ensure consistency in data modeling, the thickness d_2 of the solution layer must be at least 26.40 nm.

4. Discussion

4.1 "Bragg peak"

In reflectivity spectra of self-assembled films, Bragg reflections corresponding to the internal layer structure of the film are usually not observed.[31–33] To the best of our knowledge, it is the first time that a molecular organization in a protein foam film has been identified. Such an observation is based on the use of small angle scattering using a synchrotron source (high flux, good angular resolution) but also a well controlled protein preparation (purification/lyophilization, freshly prepared solutions). The

value of 2.64 nm is surprisingly small when one considers the size of the ovalbumin molecule ($4.5 \times 5.0 \times 7.0$ nm^3).[10,34] The protein–protein interactions are dominated by electrostatic repulsion at neutral pH and low ionic strength.[24] The interparticle distance for monomers depends on the protein concentration and is typically 10 nm in concentrated solutions,[34] much higher than the value we found. Other X-ray experiments[9] have been performed on a freestanding film of β-lactoglobulin and have shown that the protein may retain its native conformation inside the film. However these studies have been performed on a Newton black film where the aqueous core is reduced to a hydration layer.

The periodicity d was assigned by using the default (001) "Bragg peak". Another scenario might be proposed assuming that the (001) "Bragg peak" is not observed but rather there is the existence of a (002) one. In this case, the distance d becomes 5.28 nm with a protein organization $N = 5$ and is compatible with the molecular dimensions. The form factor of the mean electron density of the protein packing modulates the amplitude of the "Bragg peak" and gives the "centrosymmetric" behavior of the lamellar structure. The observation of a single reflection does not us allow to describe the form factor. Similar SAXS investigations[35] have shown that some self-assembly systems are influenced by the molecular concentration or the water content. Proteins with equivalent molecular weight may be confined in lamellar structure, with a size of 2.3 nm.[35] But we cannot exclude the hypothesis that ovalbumin may partially lose its globular conformation with tertiary structure modifications. To go deeper into the understanding of the molecular alignment, it would be useful to pursue these synchrotron studies by changing the ionic strength and pH and to identify the structural changes undergone by the protein in the film.

Some SAXS tests were performed by doubling the ionic strength of the solution. Some additional peaks appear only inside the spike but the position of these peaks is highly variable from one film to another and the shape is not described by the Laue function. The reduction of the electrostatic repulsion should favor the formation of a percolation network (clusters of aggregates) within the film. Similar results were obtained with a high concentration of protein (30 g L^{-1}).

4.2 Kiessig fringes

The fitting of the synchrotron data by the "five-layer" model gave a thickness $d_2 = 27.6 \pm 0.3$ nm for the solution layers. The ratio of the electronic density ρ_1/ρ_2 and the thickness d_1 of the monolayer are found to be equal to 1.2 ± 0.1 and 1.5 ± 0.3 nm respectively ($\chi^2 = 120$, which leads to a reduced $\chi^2 = 0.46$). The value of the parameter χ^2 is large because of a rough description of the background. Knowing the structural parameters of ovalbumin,[10,34] it means that part of the molecule is identified on the interfacial layer. Taking into account these results and the molecule numbers in each layer, we can conclude that the lateral organization is different in the air/solution interface and inside the film. The fraction of proteins contained in the film plane would result in a 6% lower electronic density at the interface than inside the film.

Other synchrotron reflectivity experiments performed on the ID10B beamline (ESRF, Grenoble, France) have shown an adsorbed layer with a thickness of 1.5 nm that is markedly affected by aging due to slow conformational changes of the protein molecules.[36] However, the existence of a single layer (or thin layer with thickness d_1) in the middle of the film is a surprising result. To correctly describe the minimum Kiessig fringes, it was imperative to introduce this layer, whose electron density is close to that of the adsorbed layer. If we describe the inner layer (thickness d_2) by a molecular structure, this implies that an even number of molecules (here 10 for 2.64 nm periodicity) are arranged in pairs with a defect caused by a single molecule (layer denoted 1). Such a model was proposed to describe surfactant bilayers in a foam film beyond the critical micellar concentration, with intermolecular hydrophobic interactions (stratification).[37,38]

The remaining question is how to apply such a description for globular proteins with hydrophobic and hydrophilic parts that are not separately identified. Stratification is a general phenomenon for thin films formed from concentrated colloidal dispersions.[39,40] An oscillatory structural (attraction/repulsion) force becomes apparent when the particle density inside the film is higher than in the meniscus, by about 0.2 vol%. Despite the low bulk concentration of protein (10 g L^{-1}) corresponding to an average of 1.36×10^{-4} molecules nm^{-3}, it appears that the effective concentration in the film is much more important and may result from the drainage effect. This assumes that the water is principally contained in the Plateau border (menisci). The concentration difference between the film and the menisci should induce significant osmotic pressure. An effective concentration in the film of about 150 g L^{-1} may induce an osmotic pressure of about 0.5 bar,[41] sufficient to generate a modification of the electronic density inside the molecule or an unfolding protein with changes in tertiary structure (Gibbs free energy estimated at 220 kJ mol^{-1}). To ensure confined self-assembly of amphiphilic molecules within the film, the secondary structure of the protein should be conserved.[42]

As the modeling of Kiessig fringes and "Bragg peak" are uncorrelated, the electronic density of solution layers ρ_2 was arbitrarily set at 1. By using a Fourier transform of the electron-density profile perpendicular to the interface, it is possible to analytically calculate the reflectivity intensity by correlating Kiessig fringes and the "Bragg peak" taking into account the form factor of the protein molecule. The coupling between these two phenomena may result in a shift and modulation of the "Bragg peaks". The peak shift is not observed here and such a calculation is only relevant if the boundaries of the layers are well defined with regularity of the stratification.[43] In our case, the polydispersity in molecule size resulting from the partial unfolding leads to an average thickness d_2 of the two reference layers and the reflectivity intensity is simply the sum of two intensities arising separately from Kiessig oscillations and a "Bragg peak". The model proposed here may be incomplete but, unlike a classical reflectivity experiment for which the orientation of the wave scattering vector is controlled, the intrinsic curvature of the film probed by the X-ray beam defines the angle distribution.

Some complementary experiments performed under different conditions (line SWING, detector distance 1.201 m, acquisition time 25 ms) show that the films inside the bamboo foam have almost the same average thickness. Fig. 6 is an example of data

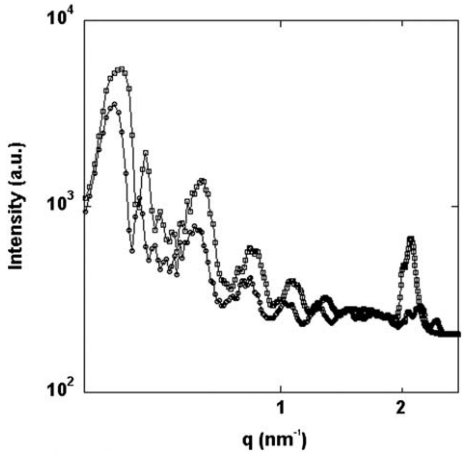

Fig. 6 The integration of synchrotron experimental data along the spike, from a filtered ovalbumin solution (0.45 μm) at pH 7 (circles) and at pH 5 (squares). The peak at 2 nm^{-1} is not a "Bragg peak" (see text).

from a filtered ovalbumin solution (0.45 μm). The "Bragg peak" is very sensitive to the film orientation relative to the beam but also the quality of the protein solutions used. If the solution is not filtered enough, the stratification within the film is broken by defects generated by the aggregates. A test at pH 5 (ionic strength 88.7 mM) showed that the diffraction pattern is very similar to that obtained at pH = 7. The film has almost the same thickness: the Kiessig fringes are superimposed. The peak at 2 nm^{-1} seems to be related to aggregates.

The pH effects on the interfacial rheology[13] are mainly related to the protein net electric charge and to the electrostatic repulsion, which hinders intermolecular interactions when the pH is far from the isoelectric pH (4.75). At pH 5, ovalbumin is assumed to exhibit a lower structural stability, which does not affect the average thickness of the films. However, the development of intermolecular interactions should modify the molecular organization inside the film. Failure to observe the Bragg peak deserves further experiments by varying the pH and ionic strength gradually.

4.3 Aging protein film

The overall thickness of the film is 59.7 nm, which has been confirmed by thin film balance experiments (Fig. 7). Film formation and rates of drainage depend on film history. Fresh ovalbumin films are more stable if the solution is filtered. By applying external pressures of about 1 kPa to induce drainage, the film was thinned and took on a gray appearance. According to Newton's colors, the film thickness must be between 50 and 60 nm. Aging of the film has been observed over time (for one hour): surface aggregation appeared at the micron scale, suggesting that the film became heterogeneous in thickness. Studying aged films has dramatic effects for reflectivity experiments generating a progressive disappearance of well-defined oscillations over time. For synchrotron experiments, the acquisition time was so short (10 ms) that film aging is unlikely to occur. A series of scans performed at the same point of a film have shown that ovalbumin is not denatured by the high flux of synchrotron source. However it is possible that aging effect may have damaged the in-house X-ray acquisitions for which the acquisition time was longer (15 min) and made it difficult to get a good signal to noise ratio. The in-house X-ray flux on the sample is about 3×10^8 ph s^{-1} to 10^{12} ph s^{-1} for the SWING line, which also explains the failure to observe the "Bragg peak" in the scattering pattern. Taking the parameters established by fitting the synchrotron data, Fig. 3 shows a fairly good description of the in-house X-ray results.

The data could also be fitted by taking a film thickness of 30 nm *i.e.* half the thickness found in our model by simply using the "three-layer" model.[22] However, the minima of the fringes would have been badly described. We are aware that our model is rather simple compared to those developed for specific measurements of reflectivity.[26–30,43] However, the description of the oscillations by setting the positions of the maxima and minima is clearly mainly due to the existence of a five layer model. The oscillation profiles at larger q may be related to the effect of roughness that we have neglected. A study of the variation of the diffraction spectra with the temperature might have been helpful but is not an option for films greatly destabilized at high temperature. Nevertheless, the similarity between the in house spectra ($T = 20$ °C) and the synchrotron experiment ($T =$ 25 °C) indicates that the temperature does not have a major influence on the spectra.

5. Conclusion

SAXS experiments with drained films stabilized by ovalbumin (pH 7) highlighted the existence of stratification inside the film with well-defined organization. The stratification also indicates that the effective concentration of molecules confined in the film is much higher than in the initial bulk concentration and that the majority of water is contained in the Plateau border. The observation of Kiessig fringes by in-house X-ray and synchrotron radiation have shown that the films are thin with an average

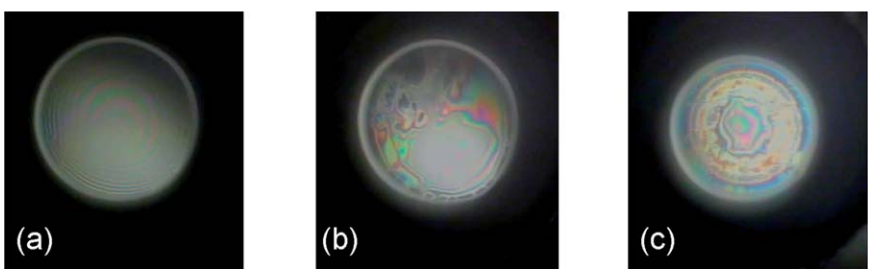

Fig. 7 Top views of ovalbumin thin films, obtained with the thin film balance apparatus after aging for (a) 10 min, (b) 35 min, (c) 1 h 35 min.

thickness of 60 nm. For each experiment, solutions of highly purified protein were freshly prepared to eliminate any problem of aging. Considering the available data about ovalbumin foaming properties as affected by, *e.g.*, the protein net charge, it seems interesting to use SAXS to study the structure of the film in various pH and ionic strength conditions. It is likely that the molecules lose their tertiary structures if the observed "Bragg peak" is attributed to the first order one. However, we cannot exclude that the molecule retains its configuration: the non observation of a (001) "Bragg peak" would then be explained by a modification of the mean electron density of the molecular packing

Acknowledgements

We are grateful to Hervé Tabuteau for the useful discussions, and Marie Postic, Federico Casanova and Thomas Bizien for technical assistance.

References

1 E. Dickinson, *An Introduction to Food Colloids*, Oxford University Press, 1992.
2 P. J. Atkinson, E. Dickinson, D. S. Horne and R. M. Richardson, *J. Chem. Soc., Faraday Trans.*, 1995, **91**, 2847.
3 A. H. Martin, K. Grolle, M. A. Bos, M. A. Stuart and T. van Vliet, *J. Colloid Interface Sci.*, 2002, **254**, 175.
4 V. Lechevalier, T. Croguennec, S. Pezennec, C. Guérin-Dubiard, M. Pasco and F. Nau, *Food Chem.*, 2005, **92**, 9.
5 T. Dimitrova, F. Leal-Calderon, T. D. Gurkov and B. Campbell, *Langmuir*, 2001, **17**, 8069.
6 G. Yampolskaya and D. Platikanov, *Adv. Colloid Interface Sci.*, 2006, **128**, 159.
7 L. G. C. Pereira, C. Johansson, C. J. Radke and H. W. Blanch, *Langmuir*, 2003, **19**, 7503.
8 B. Rullier, M. A. V. Axelos, D. Langevin and B. Novales, *J. Colloid Interface Sci.*, 2010, **343**, 330.
9 V. Petkova, C. Sultanem, M. Nedyalkov, J. J. Benattar, M. E. Leser and C. Schmitt, *Langmuir*, 2003, **19**, 6942.
10 P. E. Stein, A. G. W. Leslie, J. T. Finch and R. W. Carell, *J. Mol. Biol.*, 1991, **221**, 941.
11 E. H. Lucassen-Reynders, J. Benjamins, in *Food emulsions and foams. Interfaces, interactions and stability*, ed. E. Dickinson, J. M. Rodriguez-Patino, Royal Society of Chemistry, Cambridge, 1999, p 195.
12 L. Razumovsky and S. Damodaran, *J. Agric. Food Chem.*, 2001, **49**, 30803086.
13 A. Renault, S. Pezennec, F. Gautier, V. Vié and B. Desbat, *Langmuir*, 2002, **18**, 6887.
14 N. Kitabatake and E. Doi, *J. Agric. Food Chem.*, 1987, **35**, 953.
15 N. Pittet, P. Boltenhagen, N. Rivier and D. Weaire, *Europhys. Lett.*, 1996, **35**, 547.
16 V. Carrier, S. Hutzler and D. Weaire, *Colloids Surf., A*, 2007, **309**, 13.
17 M. A. V. Axelos and F. Boué, *Langmuir*, 2003, **19**, 6598.
18 M. H. Ropers, B. Novales, F. Boué and M. A. V. Axelos, *Langmuir*, 2008, **24**, 12849.
19 I. Schmidt, B. Novales, F. Boué and M. A. V. Axelos, *J. Colloid Interface Sci.*, 2010, **345**, 316.
20 J. Etrillard, M. A. V. Axelos, I. Cantat, F. Artzner, A. Renault, T. Weiss, R. Delannay and F. Boué, *Langmuir*, 2005, **21**, 2229.
21 E. Terriac, J. Emile, M. A. V. Axelos, I. Grillo, F. Meneau and F. Boué, *Colloids Surf., A*, 2007, **309**, 112.
22 E. Terriac, F. Artzner, A. Moréac, C. Meriadec, P. Chasle, J. C. Ameline, J. Ohana and J. Emile, *Langmuir*, 2007, **23**, 12055.
23 T. Croguennec, F. Nau, S. Pezennec and G. Brulé, *J. Agric. Food Chem.*, 2000, **48**, 4883.
24 M. R. RodriguezPatino, M. D. N. Naranjo Delgado and J. A. Linares Fernandez, *Colloids Surf., A*, 1995, **99**, 65.
25 A. P. Hammersley. Scientific software FIT2D; URL:http://www.ersf.eu/computing/scientific/FIT2D.
26 P. A. Albouy and P. Valerio, *Supramol. Sci.*, 1997, **4**, 191.
27 A. Braslau, P. S. Pershan, G. Swislow, B. M. Ocko and J. Als-Nielsen, *Phys. Rev. A: At., Mol., Opt. Phys.*, 1988, **38**, 2457.
28 J. Daillant and O. Bélorgey, *J. Chem. Phys.*, 1992, **97**, 5824.
29 J. Als-Nielsen, D. McMorrow,*Elements of Modern X-Ray, Physics*, Wiley, New York, 2001.
30 O. Shpyrko, M. Fukuto, P. Pershan, B. Ocko, I. Kuzmenko, T. Gog and M. Deutsch, *Phys. Rev. B: Condens. Matter Mater. Phys.*, 2004, **69**, 245423.
31 G. Decher, Y. Lvov and J. Schmitt, *Thin Solid Films*, 1994, **244**, 772.
32 F. W. Embs, G. Wegner, D. Neher, P. Albouy, R. D. Miller, C. G. Willson and W. Schrepp, *Macromolecules*, 1991, **24**, 5068.
33 J. Schmitt, T. Grünewald, G. Decher, P. S. Pershan, K. Kjaer and M. Lösche, *Macromolecules*, 1993, **26**, 7058.
34 M. Weijers, E. H. A. de Hoog, M. A. Cohen Stuart, R. W. Visschers and P. A. Barneveld, *Colloids Surf., A*, 2005, **270**, 301.
35 A. Banc, B. Desbat, D. Renard, Y. Popineau, C. Mangavel and L. Navailles, *Biopolymers*, 2009, **91**, 610.
36 S. Beaufils, O. Konovalov, S. Pezennec and A. Renault, unpublished results.
37 V. Bergeron, D. Langevin and A. Asnacios, *Langmuir*, 1996, **12**, 1550.
38 P. Richetti and P. Kekicheff, *Phys. Rev. Lett.*, 1992, **68**, 1951.
39 A. D. Nikolov and D. T. Wasan, *Langmuir*, 1992, **8**, 2985.
40 K. Koczo, A. D. Nikolov, D. T. Wasan, R. P. Borwankar and A. Gonsalves, *J. Colloid Interface Sci.*, 1996, **178**, 694.
41 M. A. Yousef, R. Datta and V. G. J. Rodgers, *J. Colloid Interface Sci.*, 2001, **243**, 321.
42 P. T. Hammond, *Curr. Opin. Colloid Interface Sci.*, 2000, **4**, 430.
43 F. Rieutord, J. J. Benattar, L. Bosio, C. Blot and R. de Kouchkovsky, *J. Phys.*, 1987, **48**, 679.

